DARK MATTER IN THE GALACTIC DWARF SATELLITES

Kohei Hayashi
(Kavli IPMU)

Outline

- Properties of non-spherical dark halos in the Galactic dwarf spheroidal (dSph) galaxies
- Dark matter annihilation and decay from non-spherical dark halos in dSphs
- Future prospects

NON-SPHERICAL DARK HALO IN DSPHS

Galactic dSphs as a probe of DM

Mass to Light ratio (M/L) within stellar extent in dSphs

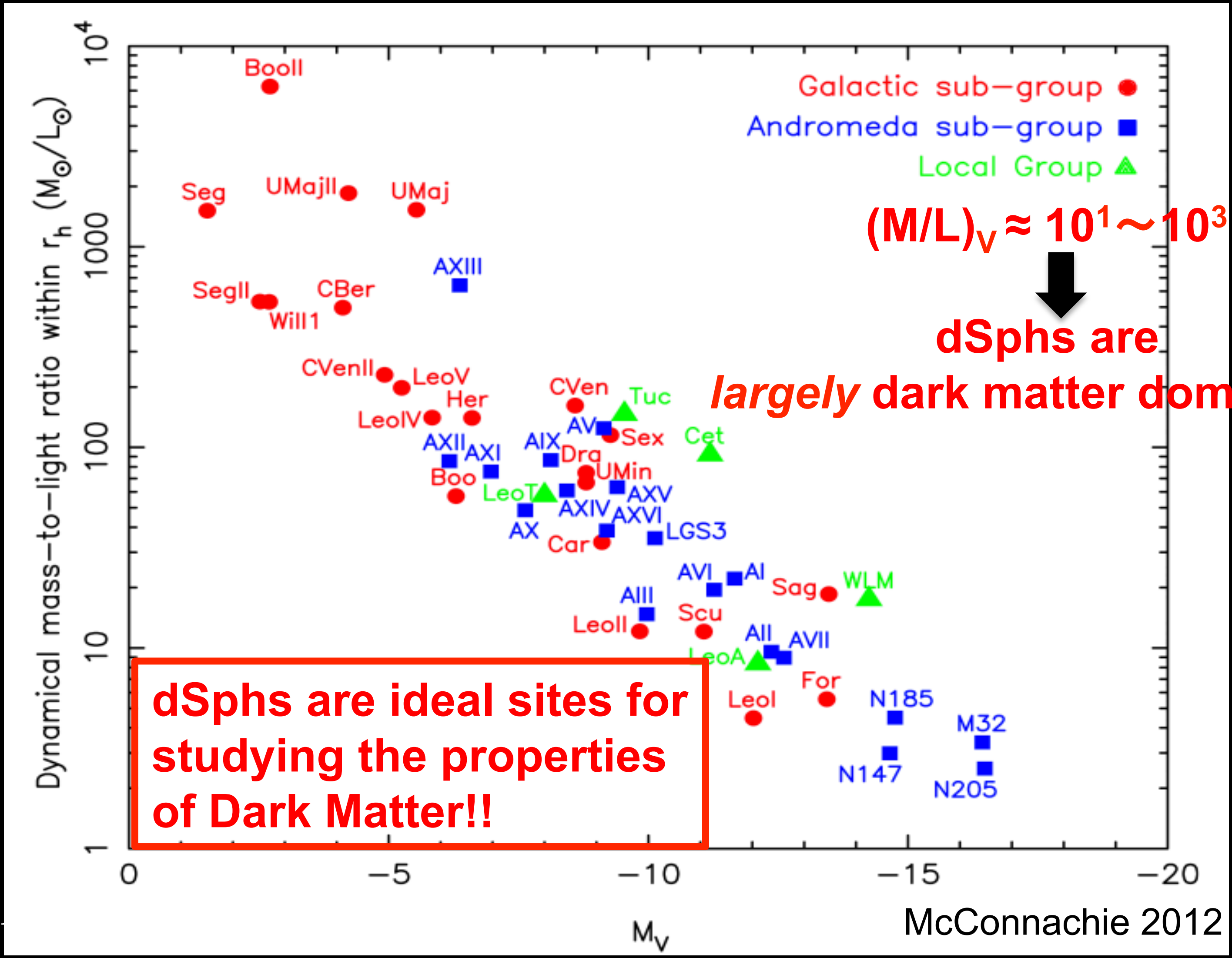

$(M/L)_V \approx 10^1 \sim 10^3$

dSphs are *largely* dark matter dominated !

dSphs are ideal sites for studying the properties of Dark Matter!!

Deriving DM profiles from spherical mass models

Spherical mass models

$$\sigma_p^2(R) = \frac{2}{I(R)} \int_R^\infty \left(1 - \beta \frac{R^2}{r^2}\right) \frac{\nu(r)\overline{v_r^2}\, r}{\sqrt{r^2 - R^2}} dr$$

$$\beta = 1 - \frac{\sigma_\phi^2 + \sigma_\theta^2}{2\sigma_r^2}$$

observed | not observed

DM halo profile:

$$\rho(r) = \frac{\rho_s}{(r/r_s)^\gamma [1 + (r/r_s)^\alpha]^{(\beta - \gamma)/\alpha}}$$

Stellar profile:

$$I(R) = \frac{L}{\pi R_{\rm half}^2} \frac{1}{(1 + R^2/R_{\rm half}^2)^2}$$

It is too simple, isn't it?

"Spherical averaged"
l-o-s velocity dispersion profiles

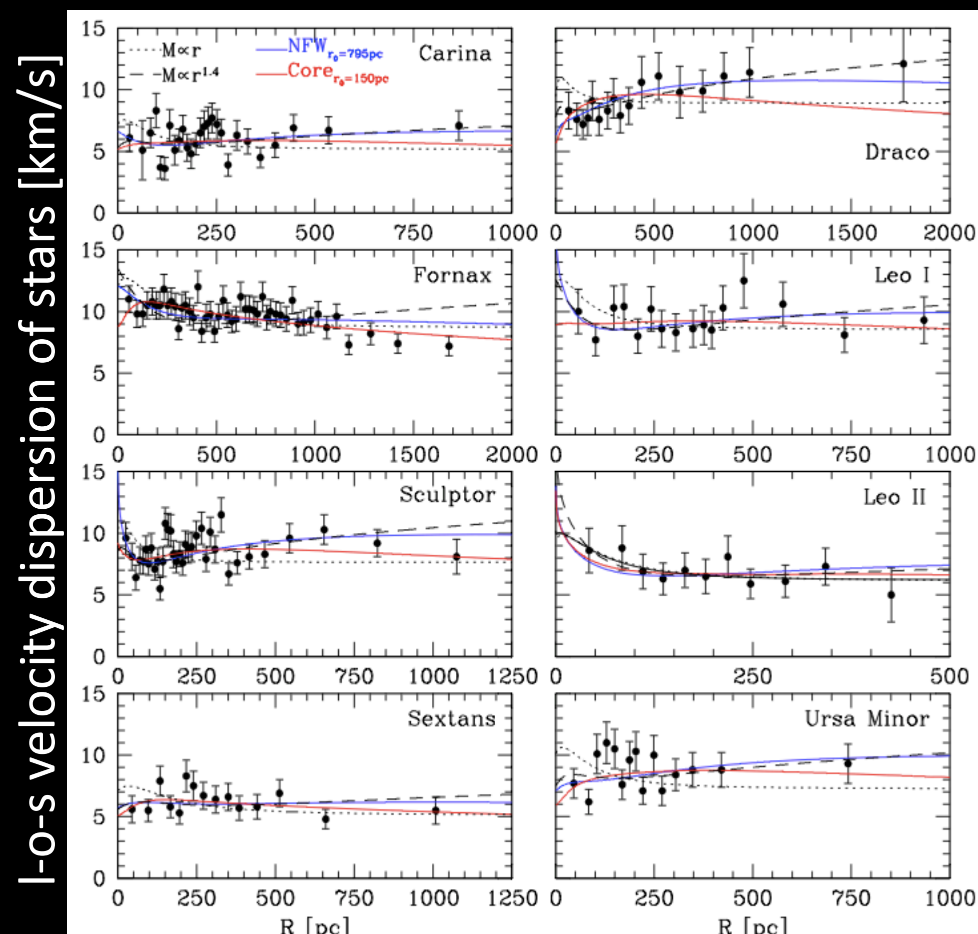

Walker+ 2009

Major systematic uncertainty: Spherical symmetry

- ✓ Stellar distributions of dSphs are actually not spherical

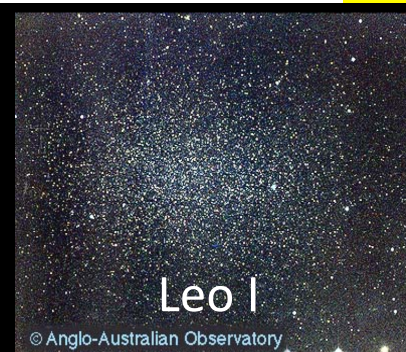

- ✓ CDM models predict non-spherical virialized halos

Springel et al.2008

Major systematic uncertainty: Spherical symmetry

✓ Stellar distributions of dSphs are actually not spherical

Construction of axisymmetric mass models for dSphs to obtain plausible limits on their density profiles and shapes of their DM halos (KH & Chiba 2012, 2015a, b).

Springel et al.2008

※Assumptions※

- Stellar components are in dynamical equilibrium.
- Static gravitational potential is dominated by DM.
- DSphs are considered as a collisionless system.
- Axisymmetry in both stellar and DM components.
- Velocity anisotropy, β_z, is constant.

·Axisymmetric Jeans equations

$$\overline{v_z^2} = \frac{1}{\nu(R,z)} \int_z^\infty \nu \frac{\partial \Phi}{\partial z} dz \qquad \overline{v_\phi^2} = \frac{1}{1-\beta_z}\left[\overline{v_z^2} + \frac{R}{\nu}\frac{\partial(\nu \overline{v_z^2})}{\partial R}\right] + R\frac{\partial \Phi}{\partial R}$$

$\beta_z = 1 - \overline{v_z^2}/\overline{v_R^2}$ **: velocity anisotropy**

·Luminous component

$$\nu(R,z) = \frac{3L}{4\pi b_*^3}\left[1 + \frac{m_*^2}{b_*^2}\right]^{-5/2}$$

$m_*^2 = R^2 + \frac{z^2}{q^2}$ **q : axial ratio**

$q'^2 = \cos^2 i + q^2 \sin^2 i$ **q' : projected q**

·DM-halo component

$$\rho(R,z) = \rho_0 \left(\frac{m}{b_{\rm halo}}\right)^\alpha \left[1 + \left(\frac{m}{b_{\rm halo}}\right)^2\right]^{-(\alpha+3)/2}$$

$m^2 = R^2 + \frac{z^2}{Q^2}$ **Q : DM's axial ratio**

※Assumptions※

- Stellar components are in dynamical equilibrium.
- Static gravitational potential is dominated by DM.
- DSphs are considered as a collisionless system.
- Axisymmetry in both stellar and DM components.
- Velocity anisotropy, β_z, is constant.

・Axisymmetric Jeans equations

$$\overline{v_z^2} = \frac{1}{\nu(R,z)} \int_z^\infty \nu \frac{\partial \Phi}{\partial z} dz$$

$$\overline{v_\phi^2} = \frac{1}{1-\beta_z}\left[\overline{v_z^2} + \frac{R}{\nu}\frac{\partial(\nu \overline{v_z^2})}{\partial R}\right] + R\frac{\partial \Phi}{\partial R}$$

$\beta_z = 1 - \overline{v_z^2}/\overline{v_R^2}$ **: velocity anisotropy**

Free parameters

・Luminous component

$$\nu(R,z) = \frac{3L}{4\pi b_*^3}\left[1 + \frac{m_*^2}{b_*^2}\right]^{-5/2}$$

$$m_*^2 = R^2 + \frac{z^2}{q^2}$$

q : axial ratio

$$q'^2 = \cos^2 i + q^2 \sin^2 i$$

q' : projected q

・DM-halo component

$$\rho(R,z) = \rho_0 \left(\frac{m}{b_{\rm halo}}\right)^{\alpha}\left[1 + \left(\frac{m}{b_{\rm halo}}\right)^2\right]^{-(\alpha+3)/2}$$

$$m^2 = R^2 + \frac{z^2}{Q^2}$$

Q : DM's axial ratio

New constraint on shape of dark halo in dSphs

Hayashi & Chiba (2015b)

DSph's dark halos are not spherical but flattened.

Axial ratio of DM halo: Q

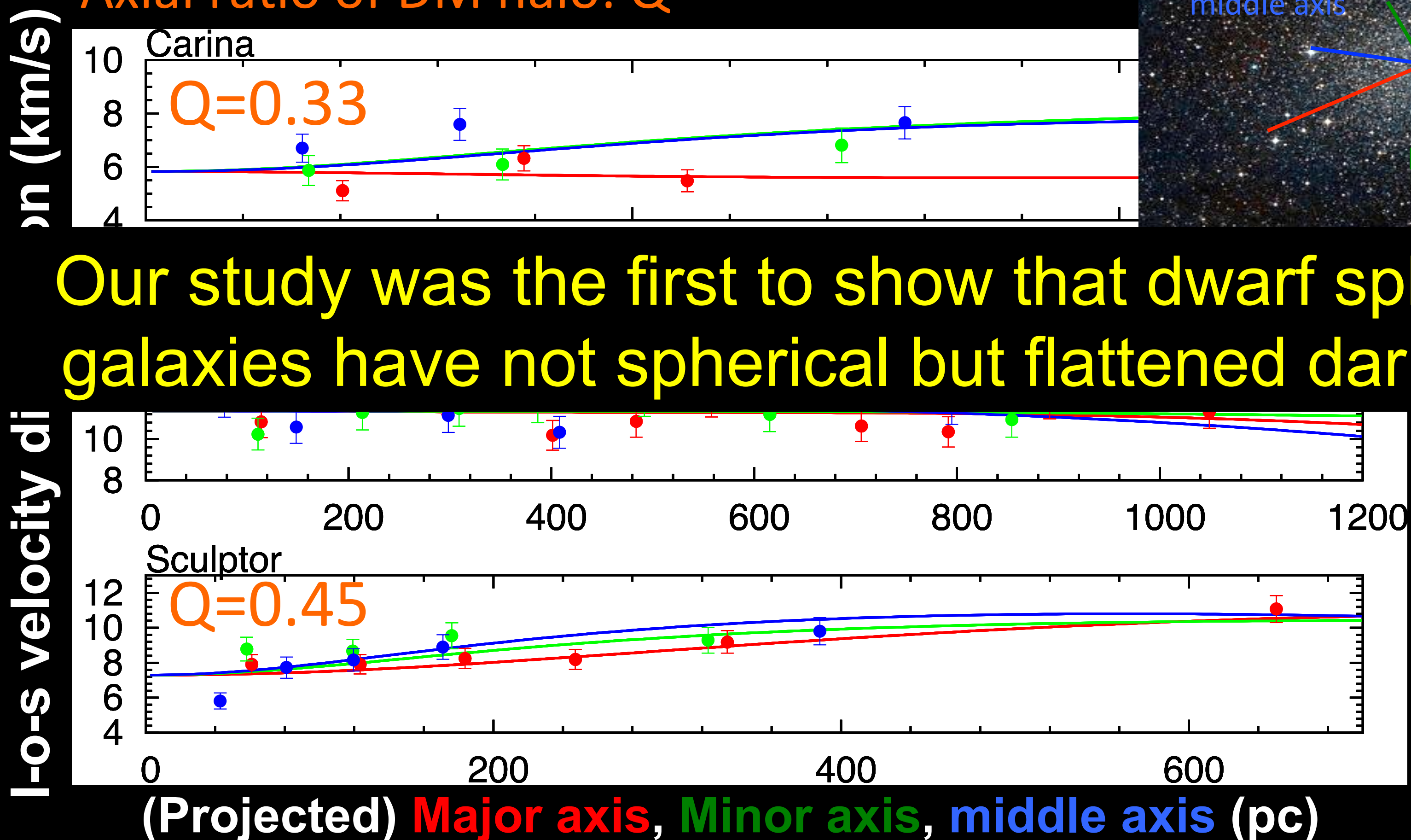

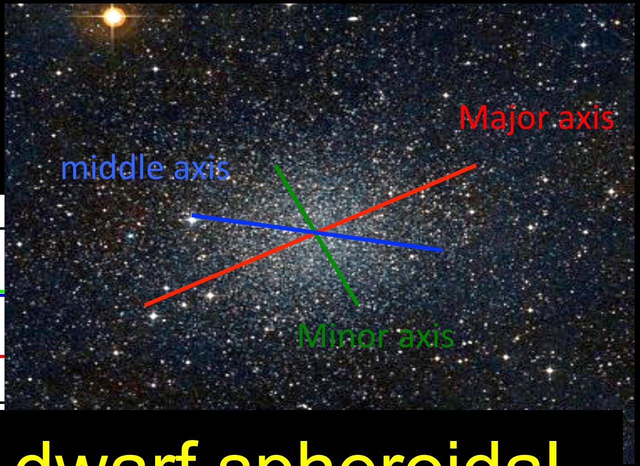

Our study was the first to show that dwarf spheroidal galaxies have not spherical but flattened dark halos!

Major systematic uncertainty: Spherical symmetry

Mass within a radius of 300 pc

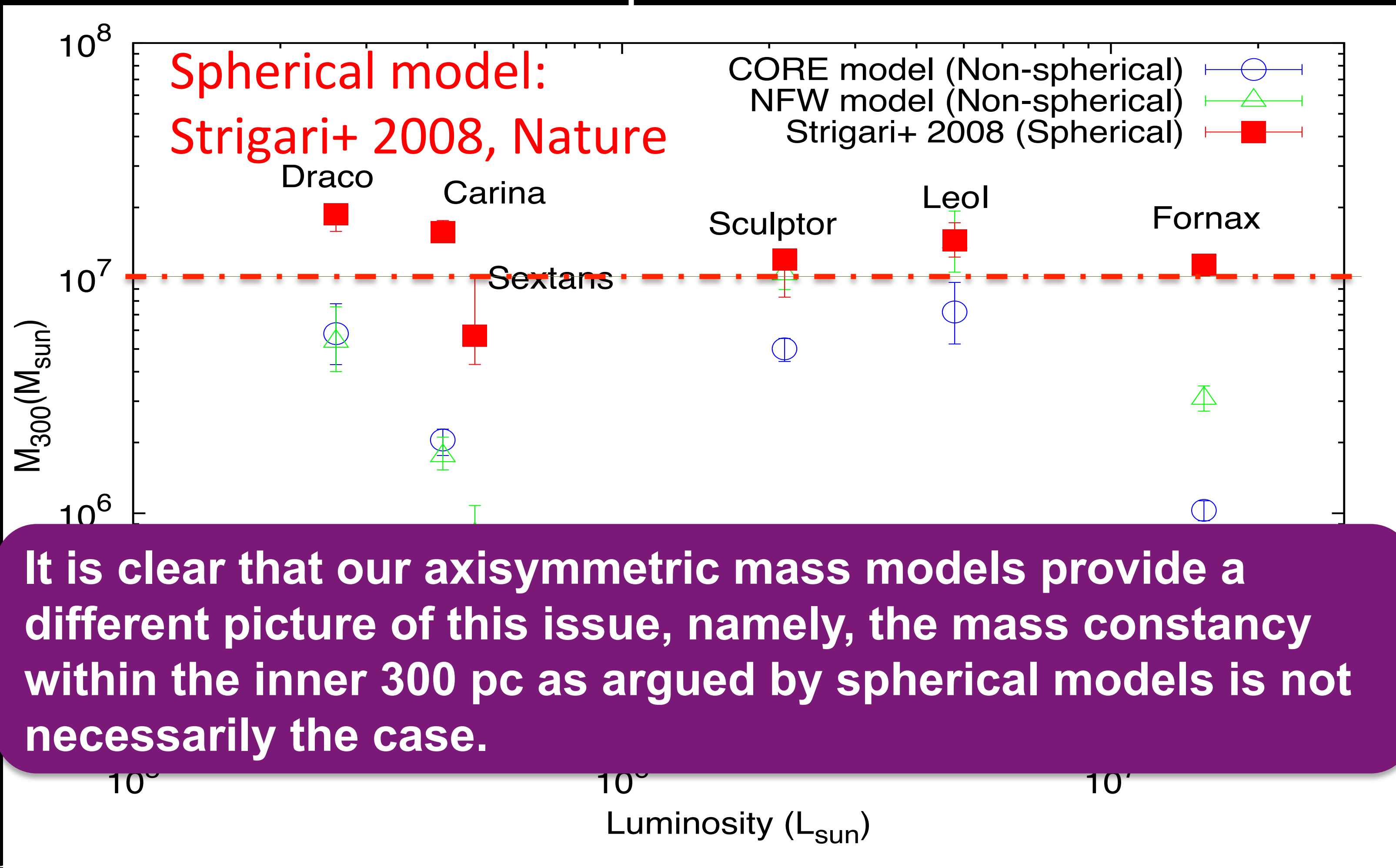

It is clear that our axisymmetric mass models provide a different picture of this issue, namely, the mass constancy within the inner 300 pc as argued by spherical models is not necessarily the case.

New universality for the DM halos

KH & Chiba(2015a,b) based on axisymmetric mass models

✓ Maximum circular velocity

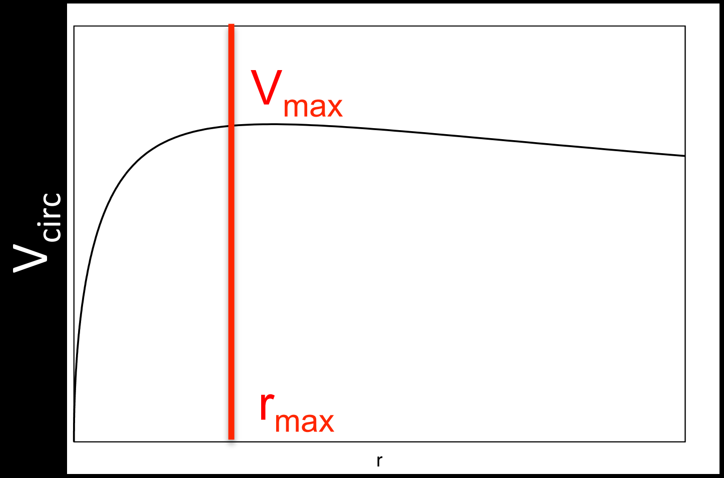

We suppose that a test particle perform circular motion in a DM halo potential.

$$V_{\rm circ}(r) = \sqrt{\frac{GM(<r)}{r}}$$

r_{max} indicates the radius of the maximum value of circular velocity, V_{max}.

✓ DM surface density within r_{max}

$$\Sigma_{V_{\rm max}} = \frac{M(r_{\rm max})}{\pi r_{\rm max}^2}$$

$$\Sigma_{V_{\rm max}} \propto \rho_s r_s$$

for NEW profiles

$$\rho(r) = \rho_s (r/r_s)^{-1}(1+r/r_s)^{-2}$$

A common surface density scale for dark halos

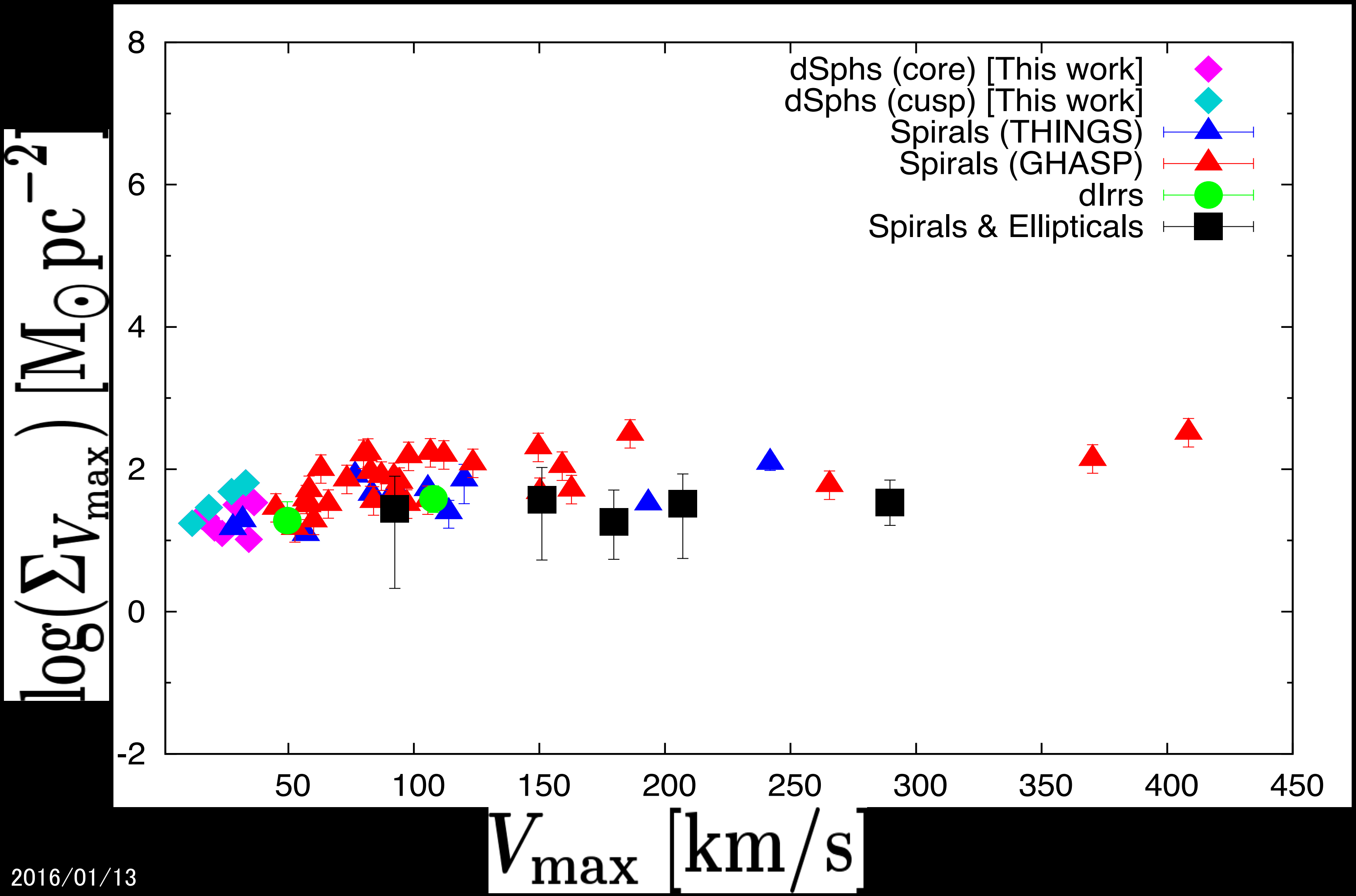

2016/01/13

A common surface density scale for dark halos

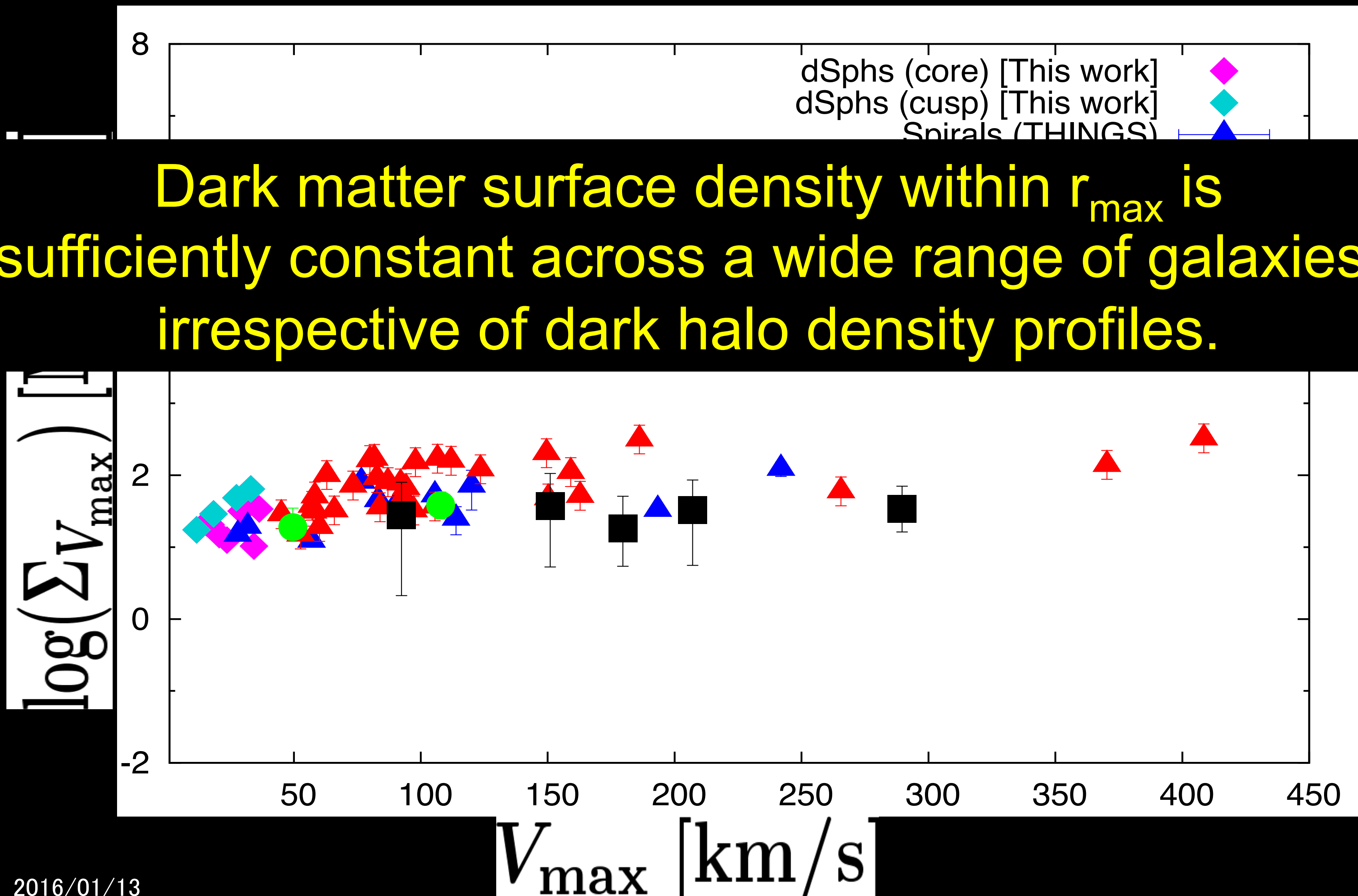

Dark matter surface density within r_{max} is sufficiently constant across a wide range of galaxies, irrespective of dark halo density profiles.

2016/01/13

Comparison with dark matter scenario

✓ At higher halo-mass range

fitting to the data!

✓ Mean surface density derived from WDM largely deviates from the observational constancy at dwarf-galaxy mass scales.

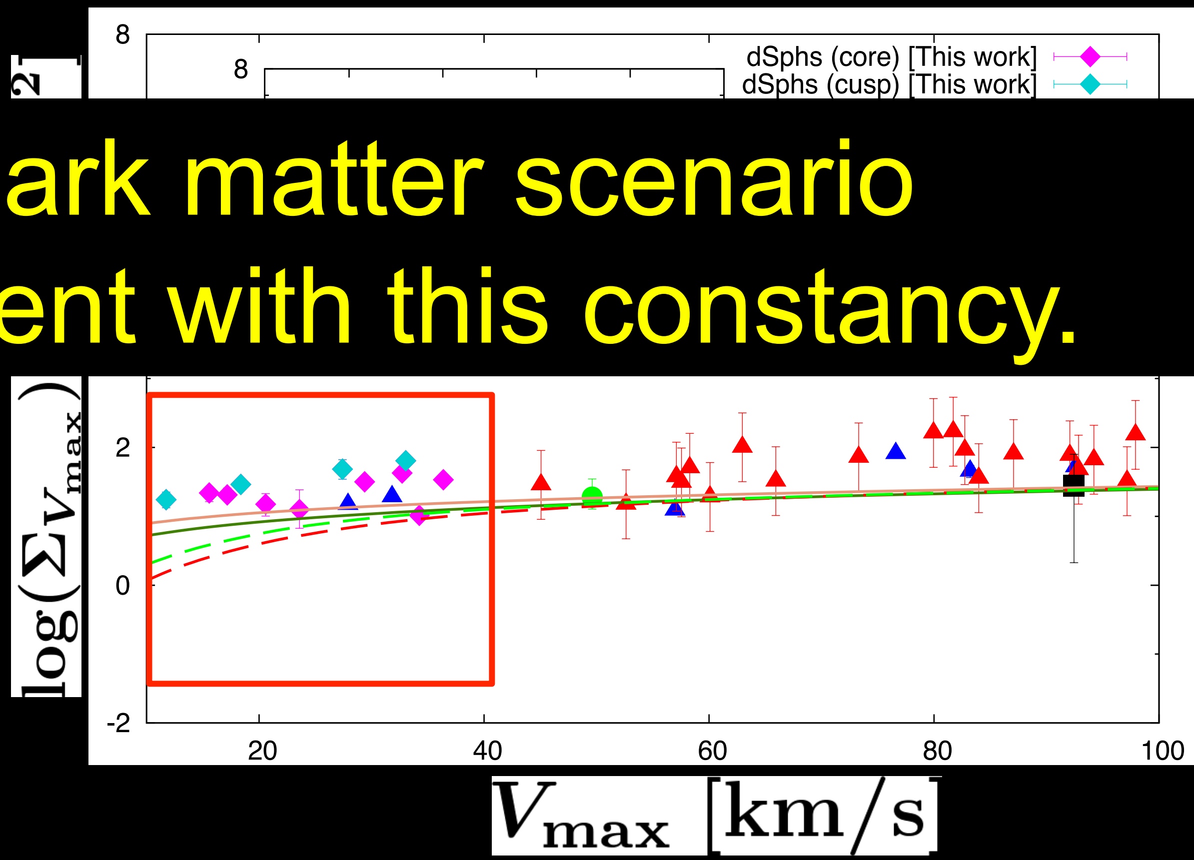

Warm dark matter scenario is inconsistent with this constancy.

Comparison with dark matter scenario

- ✓ At higher halo-mass range, this constancy for real galaxies can be naturally reproduced by both CDM & WDM, even though do not perform any fitting to the data!
- ✓ Mean surface density derived from WDM largely deviates from the observational constancy at dwarf-galaxy mass scales.

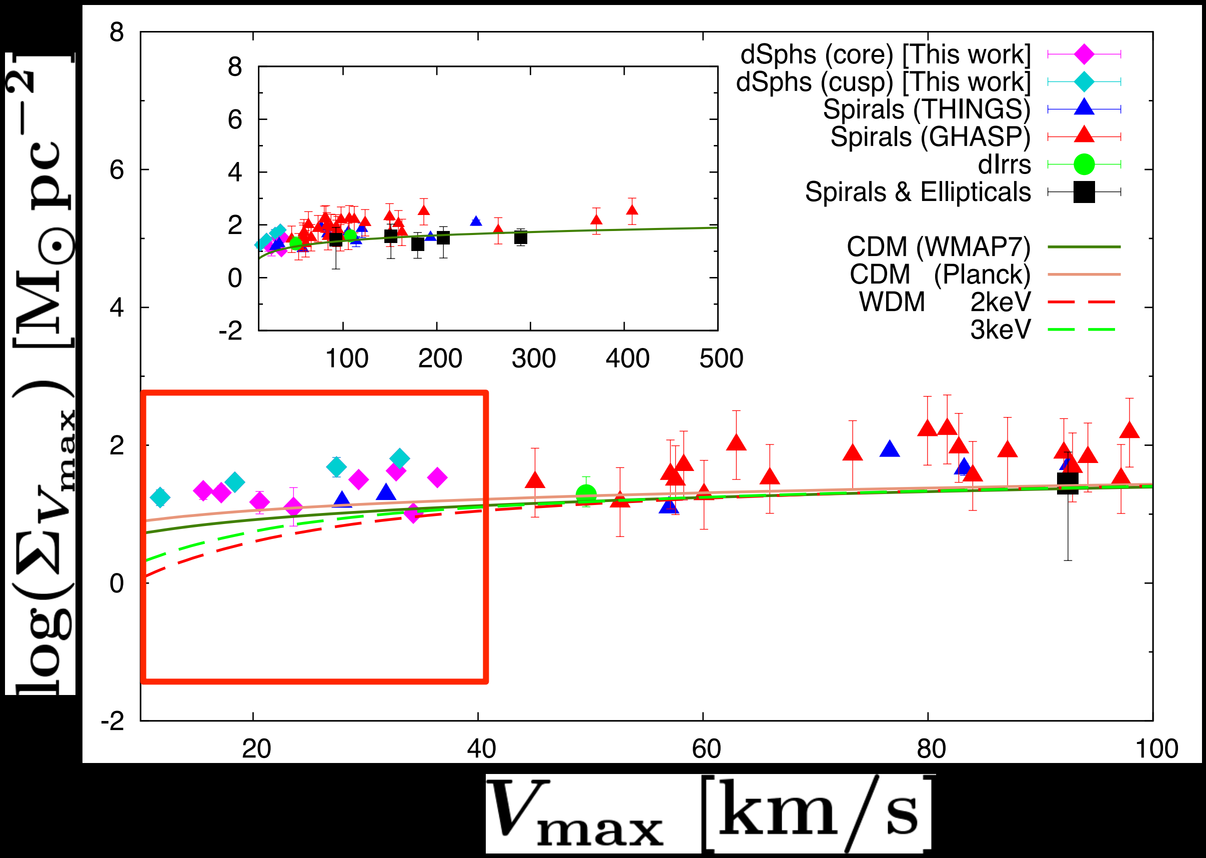

DARK MATTER ANNIHILATION AND DECAY FROM NON-SPHERICAL DARK HALO

KH, K. Ichikawa, S. Matsumoto, M. Ibe, M. N. Ishigaki & H. Sugai, 2016 (in preparation)

Indirect search for dark matter

Galactic dSphs are ideal sites for detecting a dark matter Signal !

Galactic dSphs:

- ✓ largely dark matter dominated systems (M/Ls ~ 10 to 1000)
- ✓ locate close to the Sun (about 20 to 200 kpc)
- ✓ lack of astrophysical contaminating gamma-ray sources (no gas & no current SF)

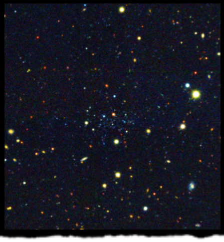

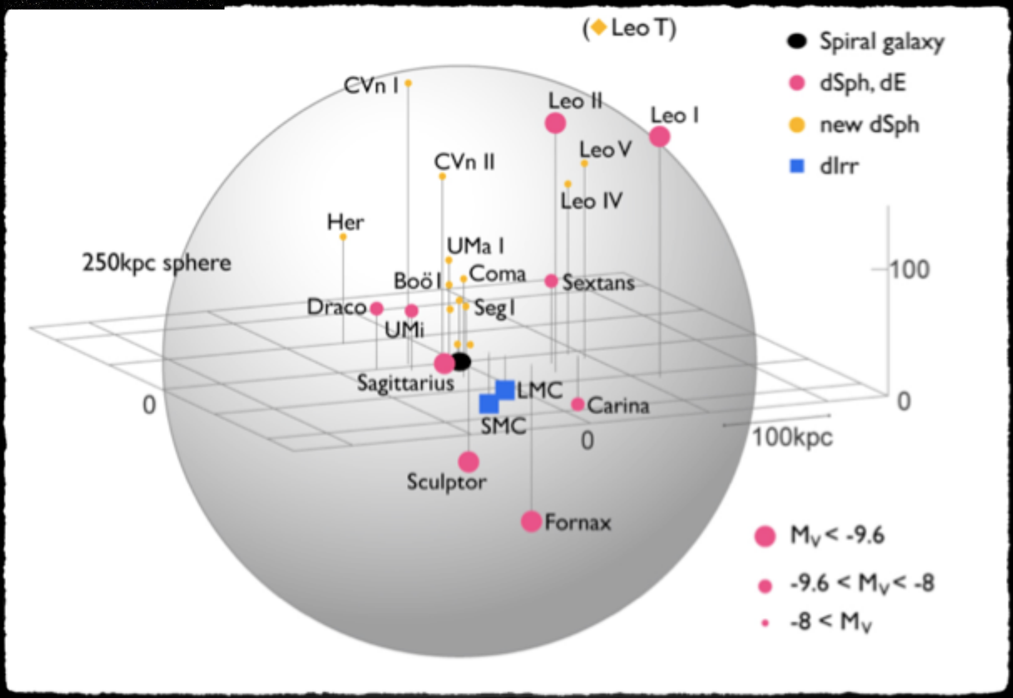

S. Okamoto PhD thesis

Upper limit on particle DM parameters

$$\Phi(E,\Delta\Omega) = \left[\frac{\langle\sigma v\rangle}{8\pi m_{\rm DM}^2}\sum_f {\rm Br}({\rm DM\,DM}\to f)\left(\frac{dN_\gamma}{dE}\right)\right]\left[\int_{\Delta\Omega} d\Omega \int_{\rm l.o.s} d\ell \rho^2(\ell,\Omega)\right]$$

Observed γ-ray flux

Theoretical predictions

Dark halo profile (J-factor)

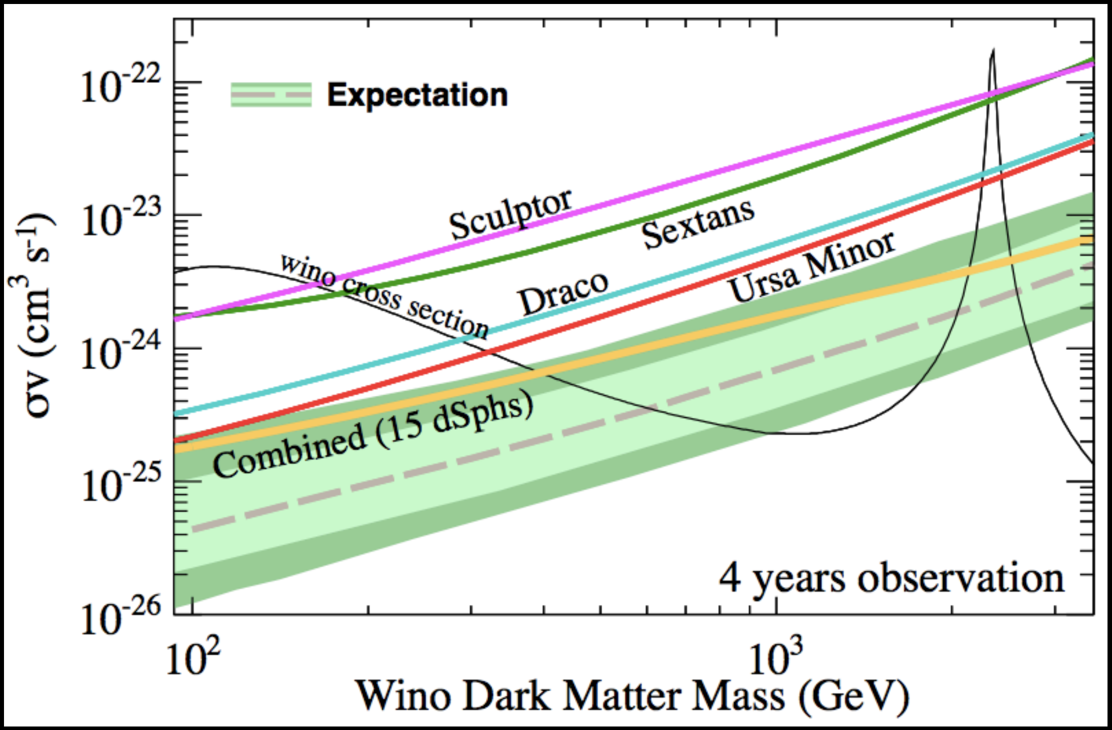

Bhattacherjee et al. 2014

To obtain further limits on properties of dark matter particle,

We need determine the dSph's dark halo structure (J-factor) more precisely !

Major systematic uncertainties on *J*

- **Non-spherical dark halo**

Most previous works estimated J values by assuming spherical mass models, even though dark halos in dSphs are not spherical but elongated (Hayashi & Chiba 2012, 2015b).

- **Foreground contaminations**

These have largely impact on determining dark halo profiles, especially ultra faint dwarfs (Bonnivard et al. 2015).

- **Data volume**

The constraints on dark halo structures in dSphs are affected largely by the lack of kinematic sample and distribution of member stars (Hayashi & Chiba 2015b).

Our targets

Axisymmetric Jeans equations

$$\overline{v_z^2} = \frac{1}{\nu(R,z)}\int_z^{\infty} \nu \frac{\partial \Phi}{\partial z} dz, \quad \overline{v_\phi^2} = \frac{1}{1-\beta_z}\left[\overline{v_z^2} + \frac{R}{\nu}\frac{\partial(\nu \overline{v_z^2})}{\partial R}\right] + R\frac{\partial \Phi}{\partial R}$$

Table 1. The observational dataset for MW dSph satellites

7 classicals

17 UFDs

Object	$N_{\rm sample}$	RA(J2000) [hh:mm:ss]	DEC(J2000) [dd:mm:ss]	M_V	$D_\odot$ [kpc]	$r_{\rm half}$ [pc]	q' (axial ratio)
Classical dwarfs							
Carina	776	06:41:36.7	−50:57:58	-9.1 ± 0.5	106 ± 6	241 ± 23	0.67 ± 0.05
Fornax	2523	02:39:59.3	−34:26:57	-13.4 ± 0.3	147 ± 12	668 ± 34	0.70 ± 0.01
Sculptor	1360	01:00:09.4	−33:42:33	-11.1 ± 0.5	86 ± 6	260 ± 39	0.68 ± 0.03
Sextans	445	10:13:03.0	−01:36:53	-9.3 ± 0.5	86 ± 4	682 ± 117	0.65 ± 0.05
Draco	468	17:20:12.4	+57:54:55	-8.8 ± 0.3	76 ± 6	196 ± 12	0.69 ± 0.02
Leo I	328	10:08:28.1	+12:18:23	-12.0 ± 0.3	254 ± 15	246 ± 19	0.79 ± 0.03
Leo II	200	11:13:28.8	+22:09:06	-9.8 ± 0.3	233 ± 14	151 ± 17	0.87 ± 0.05
Ultra faint dwarfs							
Segue 1	73	10:07:04.0	+16:04:55	-1.5 ± 0.8	32 ± 6	29^{+8}_{-5}	0.53 ± 0.10
Segue 2	24	02:19:16.0	+20:10:31	-2.5 ± 0.3	35 ± 2	35 ± 3	0.85 ± 0.13
Boötes I	37	14:00:06.0	+14:30:00	-6.3 ± 0.2	66 ± 2	242 ± 21	0.61 ± 0.06
Hercules	18	16:31:02.0	+12:47:30	-6.6 ± 0.4	132 ± 12	330^{+75}_{-52}	0.32 ± 0.08
Coma Berenices	59	12:26:59.0	+23:54:15	-3.7 ± 0.6	44 ± 4	64 ± 7	0.62 ± 0.14
Canes Venatici I	214	13:28:03.5	+33:33:21	-7.9 ± 0.5	224^{+22}_{-20}	554 ± 63	0.61 ± 0.03
Canes Venatici II	25	12:57:10.0	+34:19:15	-4.8 ± 0.6	151^{+15}_{-13}	132 ± 16	0.48 ± 0.11
Leo IV	18	11:32:57.0	−00:32:00	-5.1 ± 0.6	158^{+15}_{-14}	152 ± 17	0.51 ± 0.11
Leo V	8	11:31:09.6	+02:13:12	-5.2 ± 0.4	178 ± 10	135 ± 32	0.50 ± 0.15
Leo T	19	09:34:53.4	+17:03:05	-7.1 ± 0.3	417^{+20}_{-19}	170 ± 15	~ 1.00
Ursa Major I	39	10:34:52.8	+51:55:12	-5.6 ± 0.6	106^{+9}_{-8}	308 ± 32	0.20 ± 0.04
Ursa Major II	20	08:51:30.0	+63:07:48	-3.8 ± 0.6	32^{+5}_{-4}	127 ± 21	0.37 ± 0.05
Reticulum II	25	03:35:42.1	−54:02:57	-2.7 ± 0.1	32 ± 3	32^{+2}_{-1}	0.41 ± 0.03
Draco II	9	15:52:47.6	+64:33:55	-2.9 ± 0.8	20 ± 3	19^{+8}_{-6}	$0.76^{+0.27}_{-0.24}$
Triangulum II	13	02:13:17.4	+36:10:42	-1.8 ± 0.5	30 ± 2	34^{+9}_{-8}	$0.79^{+0.17}_{-0.21}$
Hydra II	13	12:21:42.1	−31:59:07	-4.8 ± 0.3	134 ± 10	68 ± 11	$0.99^{+0.01}_{-0.19}$
Pisces II	7	22:58:31.0	+05:57:09	-5.0 ± 0.5	~ 180	~ 60	0.60 ± 0.10

J-factor values for axisymmetric mass models

$$J \equiv \int_{\Delta\Omega} d\Omega \int_{\mathrm{l.o.s}} d\ell \rho^2(\ell, \Omega)$$

The highest J-value !

- It is found that there are differences between the values of J-factors estimated from spherical and non-spherical models, especially for UFDs.
- Errors of our work are larger than previous one because axisymmetric mass models pretty good fit to the data compared with spherical ones.
- Segue 2, Leo IV & Draco 2 have extremely low J-values because these galaxies have very small values of ρ_s and r_s due to low velocity dispersions.
- Triangulum 2 has the highest J-value, $\log_{10}(J)=21.29^{+1.62}_{-2.05}$!!

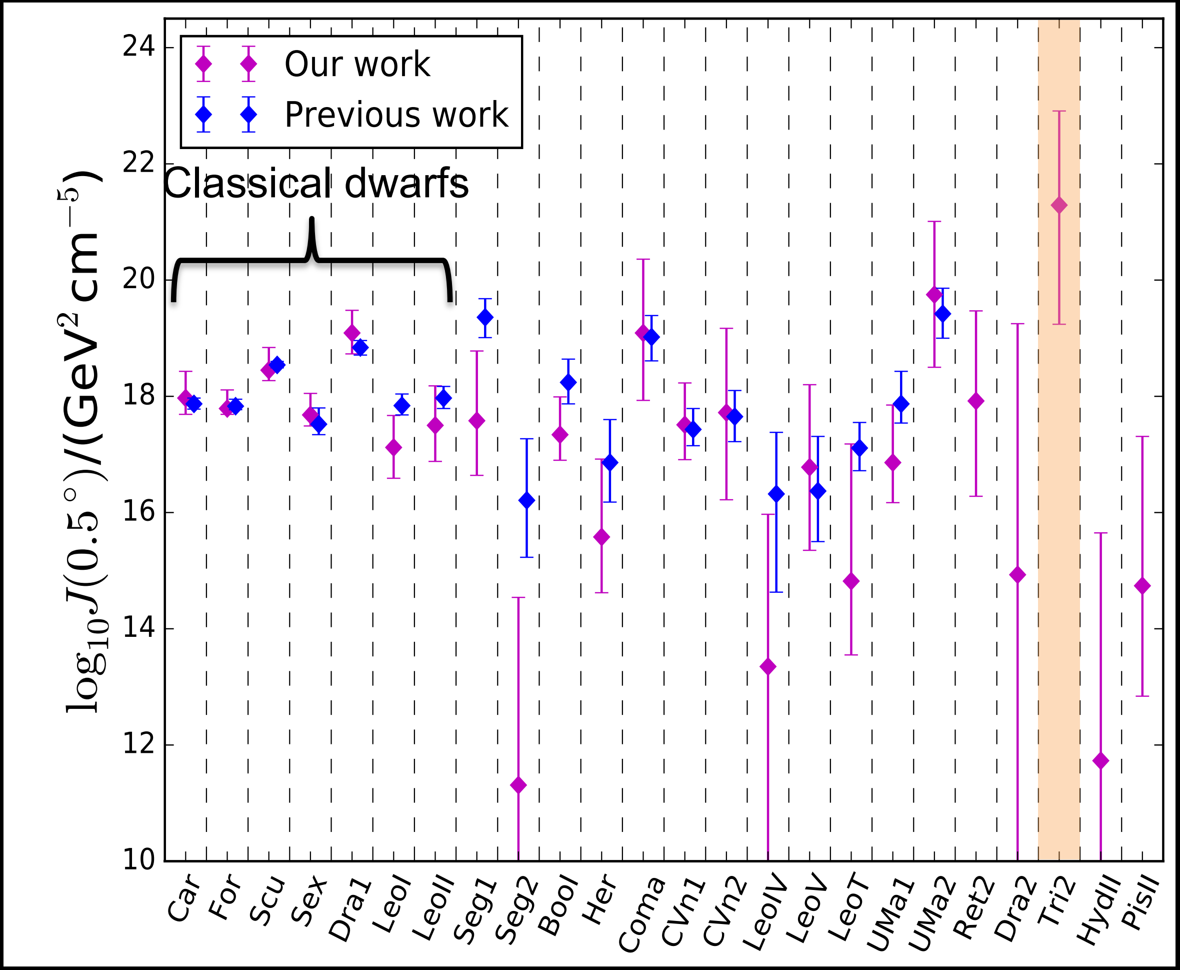

FUTURE PROSPECTS

SUBARU PRIME FOCUS SPECTROGRAPH

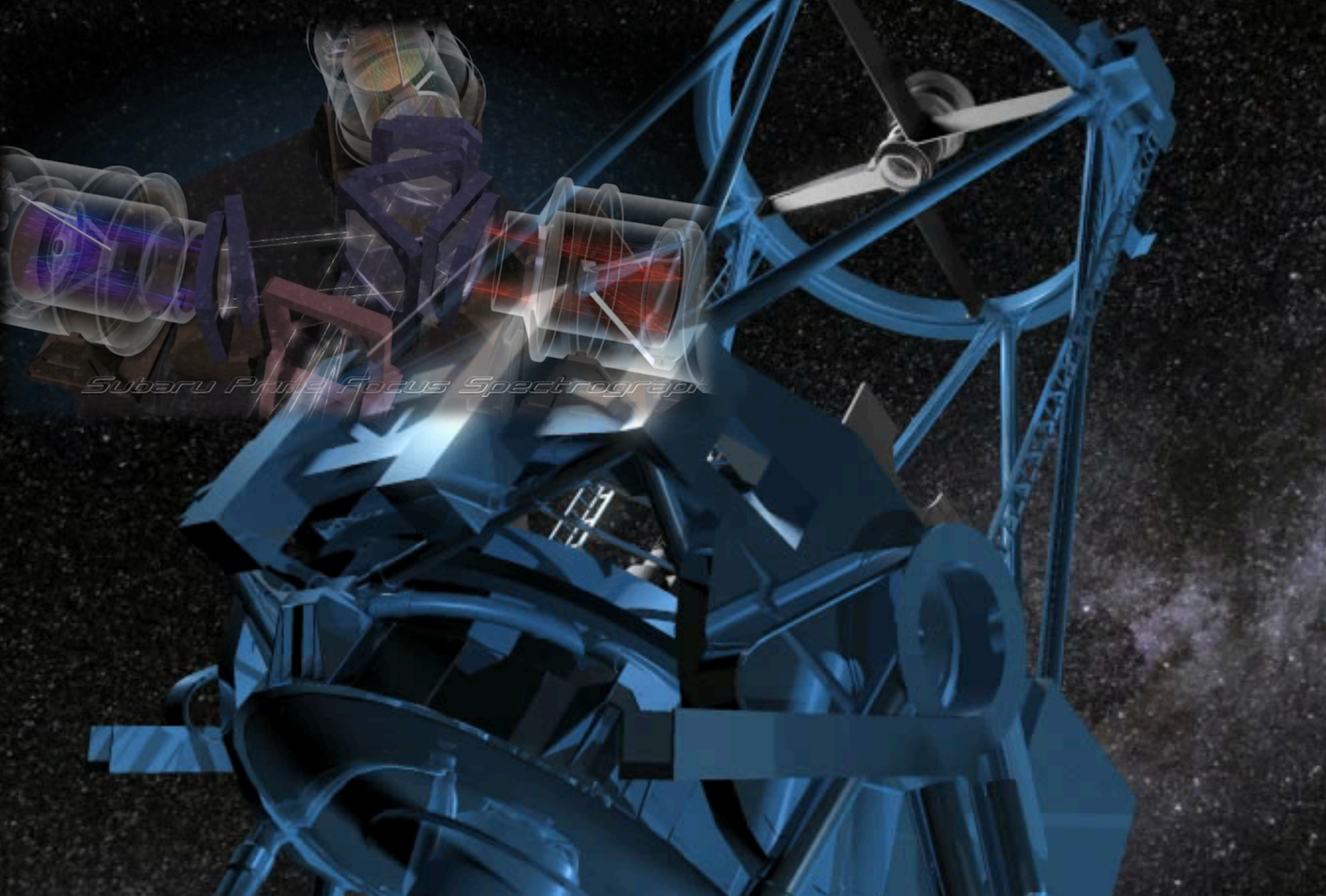

Major systematic uncertainties on *J*

- **Non-spherical dark halo**

Most previous works estimated J values by assuming spherical mass models, even though dark halos in dSphs are not spherical but elongated (Hayashi & Chiba 2012, 2015b).

- **Foreground contaminations**

These have largely impact on determining dark halo profiles, especially ultra faint dwarfs (Bonnivard et al. 2015).

- **Data volume**

The constraints on dark halo structures in dSphs are affected largely by the lack of kinematic sample and distribution of member stars (Hayashi & Chiba 2015b).

Wide & deep survey of MW dwarf galaxies w. Subaru/PFS

Blue dots: spectroscopic targets in previous work (Walker+ 2009)

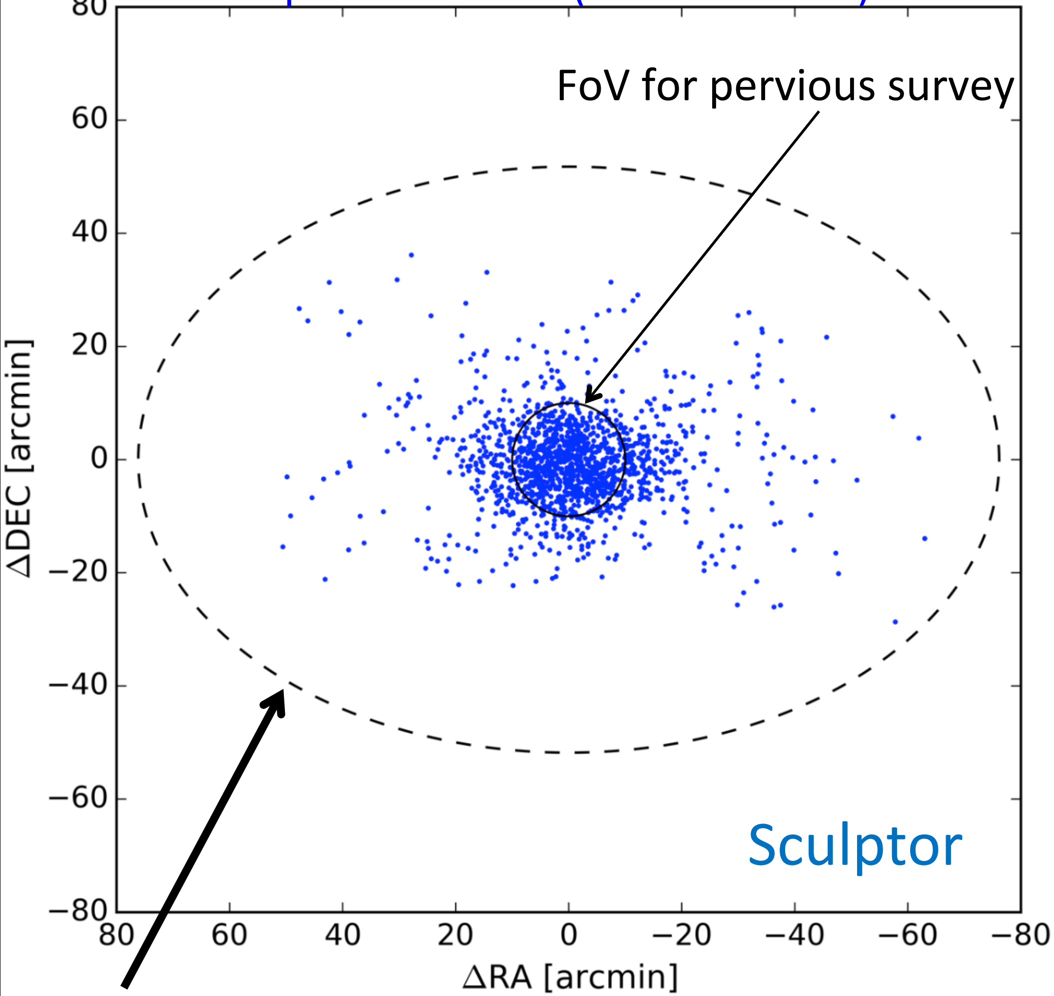

Cumulative number of observable stars (previous work by Walker+ 2009)

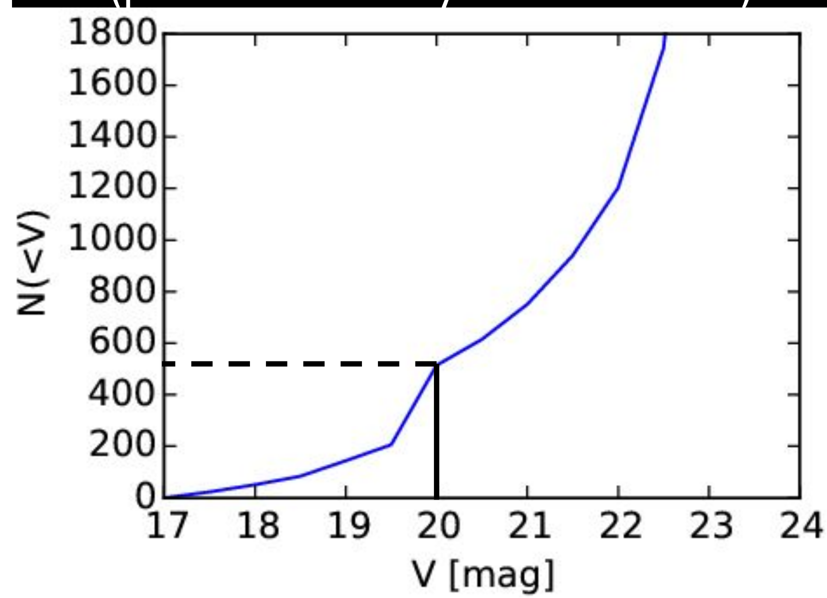

nominal boundary (r_t ~ 76'), but more member stars actually exist inside/beyond this limit.

Wide & deep survey of MW dwarf galaxies w. Subaru/PFS

Blue dots: spectroscopic targets

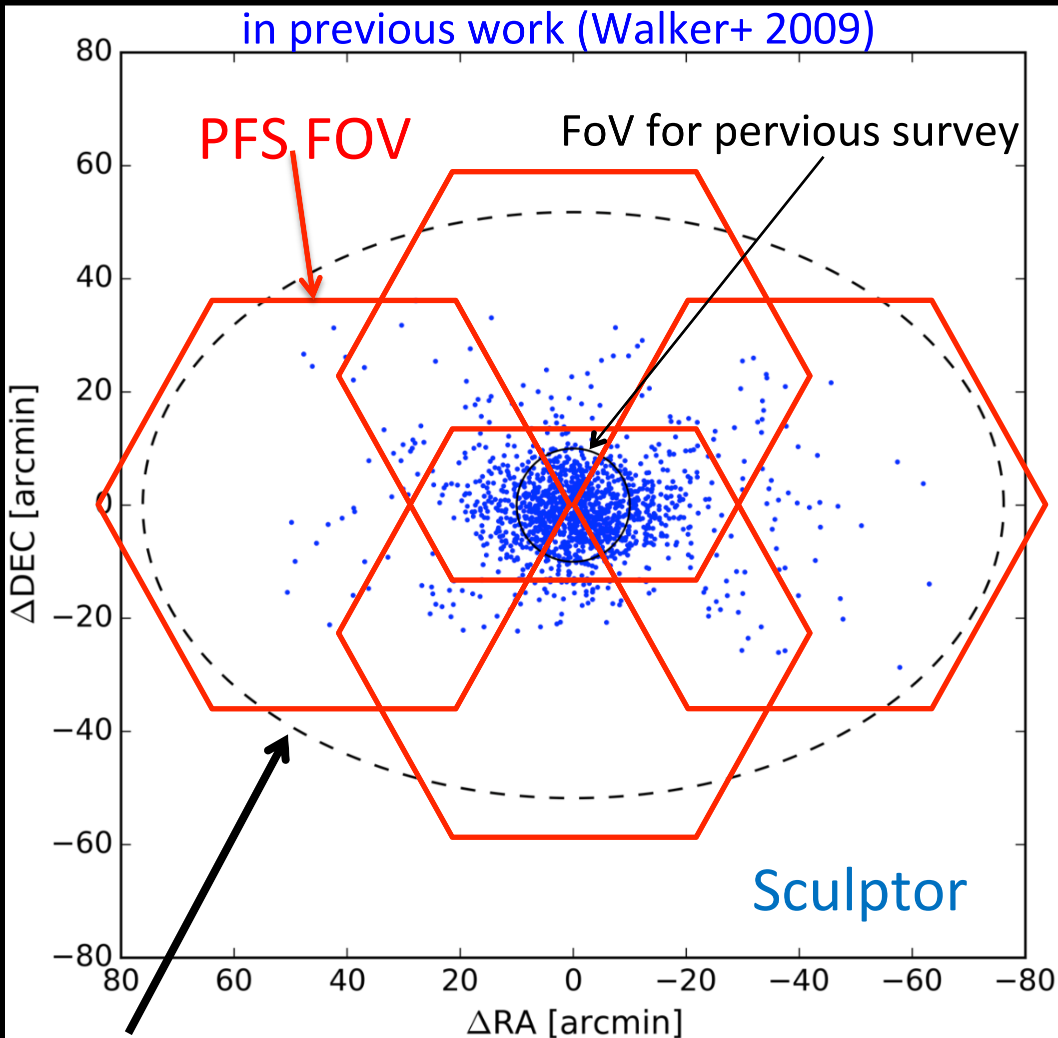

nominal boundary (r_t ~ 76’), but more member stars actually exist inside/beyond this limit.

Cumulative number of observable stars w. Subaru/PFS

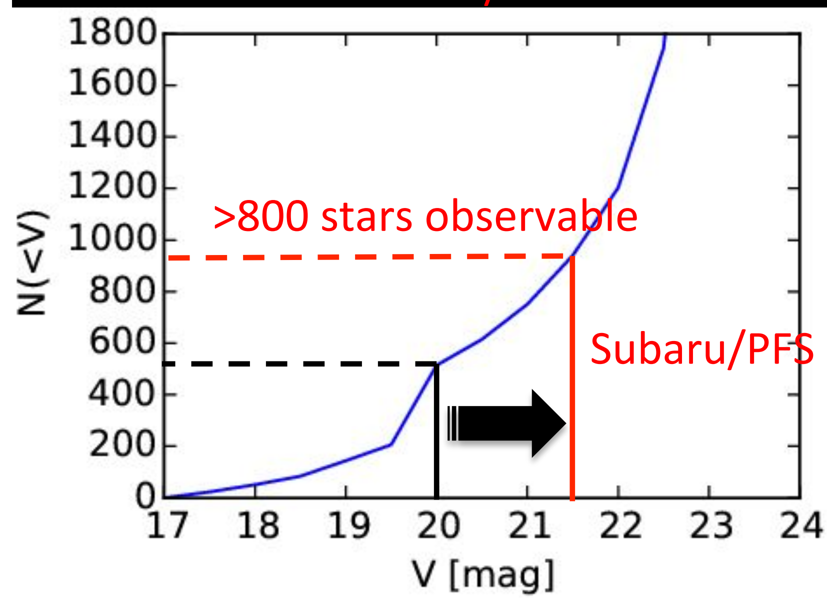

Subaru/PFS enables us to measure a large number of stellar spectra over unprecedentedly wide outer areas, <u>where DM largely dominates</u>!

⇒ Best for studying the nature of DM

PFS Survey

Precise measurement of DM Halo Profiles

K. Ichikawa

Stellar Velocity Data ⟺ DM Gravitational Potential

Fit

DM Halo: $\rho(r) = \rho_s (r/r_s)^{-1} (1 + r/r_s)^{-2}$

J-factor = $\left[\int_{\Delta\Omega} d\Omega \int_{\mathrm{l.o.s}} dl \rho^2(l, \Omega)\right]$

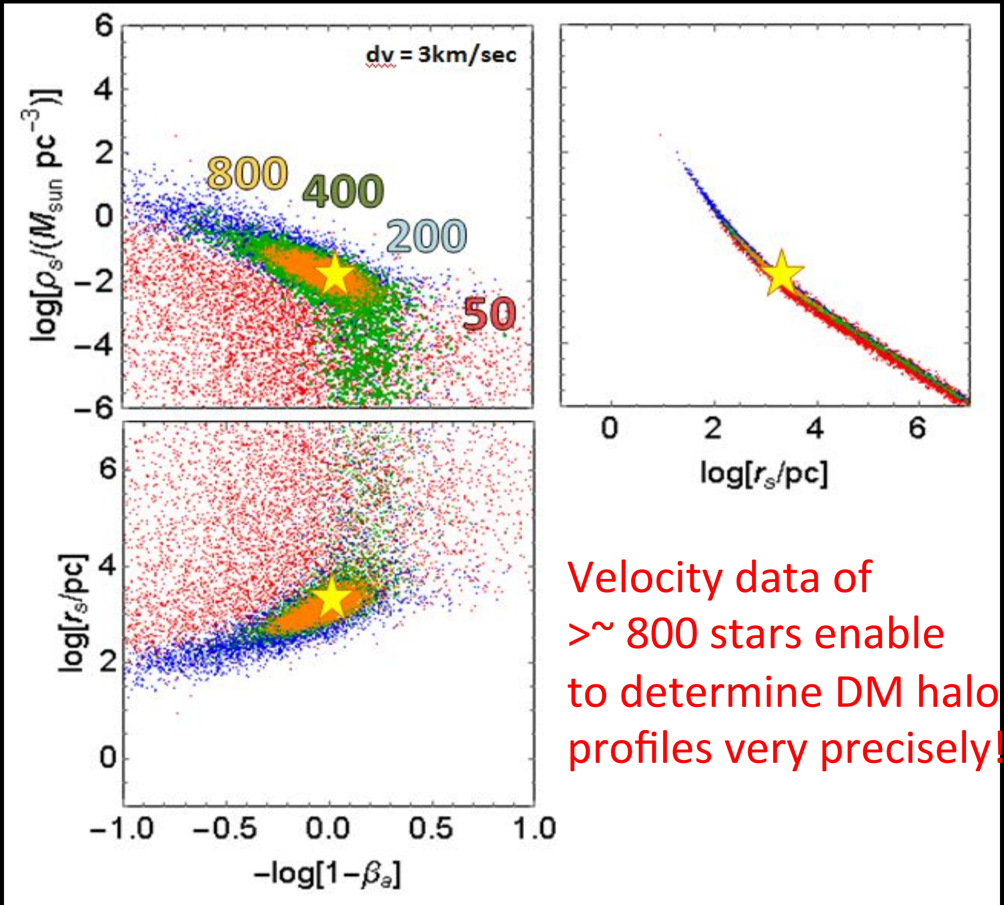

Velocity data of >~ 800 stars enable to determine DM halo profiles very precisely!

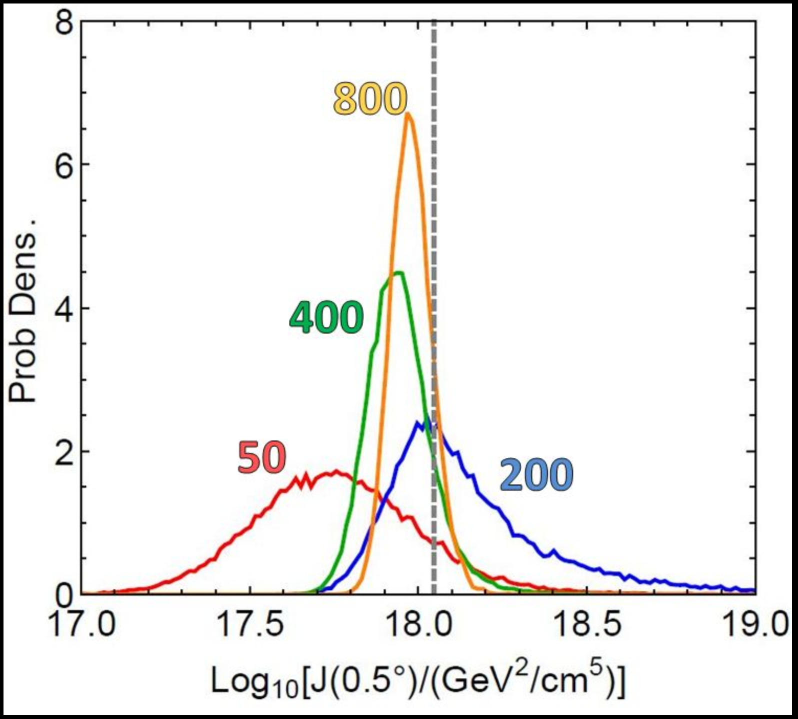

J-factor is determined very precisely!
⇒ nature of DM

SUBARU PRIME FOCUS SPECTROGRAPH

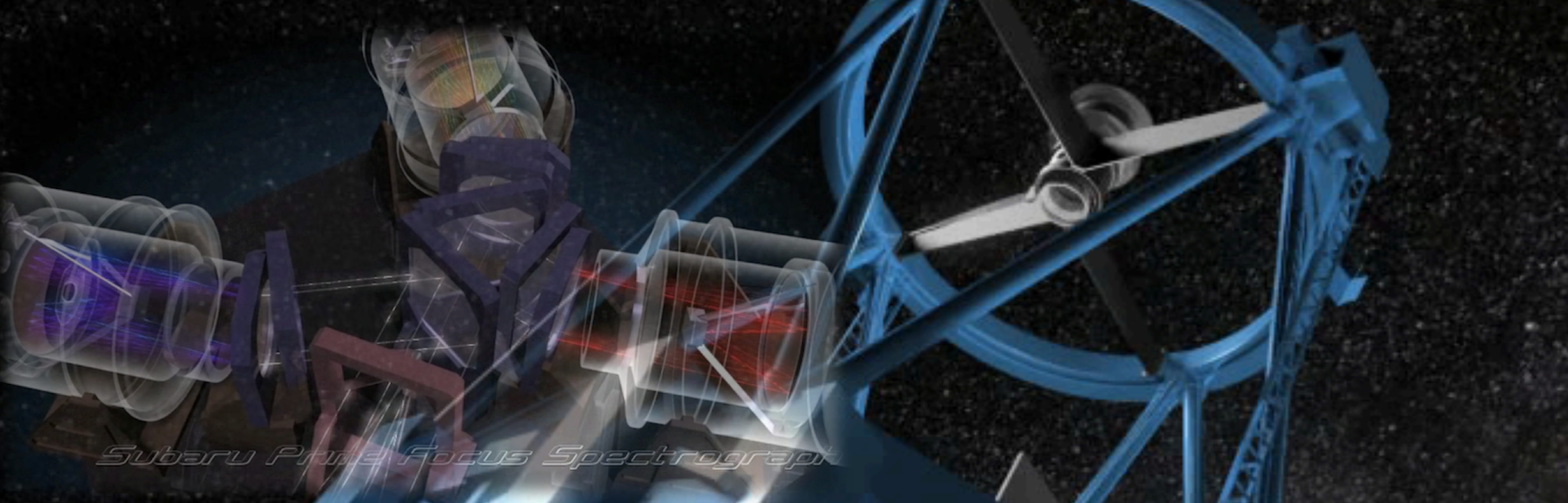

- enables us to measure a large number of spectroscopic data over wide outer area.
- provides a better determination of dark halo properties of dSphs
- can obtain severer limits on the basic properties of dark matter.

Summary & Future works

1. We have constructed axisymmetric mass models for dSphs in the MW to obtain plausible limits on the structure of their dark halos.
2. We find that the total mass of the dSphs enclosed within 300 pc varies from 10^6 $M_\odot$ to 10^7 $M_\odot$. This is quit different from the conclusion based on spherical models.
3. It is found that dark matter surface density within a radius of Vmax is nearly constant across a wide range of galaxies, and this universality is enable us to obtain the limits on particle masses of WDM scenario.
4. J-factor values are changed by assuming dark halo mass models.
5. We will investigate how much Subaru-PFS can reduce the J-factor uncertainties of non-spherical dark halos.